Synthesis and Self-Assembly of Donor−Spacer−Acceptor Molecules. Liquid Crystals Formed by Single-Component "Complexes" via Intermolecular Hydrogen-Bonding Interaction

Jianwei Xu,[†] Cher Ling Toh,[†,‡] Xueming Liu,[†] Shaofeng Wang, Chaobin He,*[,†] and Xuehong Lu[‡]

Institute of Materials Research and Engineering, 3 Research Link, Singapore 117602, Singapore, and School of Materials Engineering, Nanyang Technological University, Nanyang Avenue, Singapore 639798, Singapore

Received September 28, 2004; Revised Manuscript Received December 9, 2004

ABSTRACT: A series of donor−spacer−acceptor molecules, 4-{[*n*-(4-stilbazoyl)]alkyloxy}benzoic acid, where *n* is the number of carbon atoms in alkyloxy chain and equals to 6, 8, 10, and 12, respectively, for **6a**−**d**, were synthesized. The molecular "complexes" formed by identical **6a**−**d** molecules generated hydrogen-bonded liquid-crystalline polymers by connecting a rigid donor and a rigid acceptor of the molecules via hydrogen-bonding interaction. The thermal behaviors were studied by differential scanning calorimetry, polarizing microscopy and X-ray diffraction. The phase transition temperature of **6a**−**d** on both cooling and heating decreased steadily with the increase in length of the spacer. The hydrogen-bonding interaction in **6a**−**d** was investigated by X-ray photoelectron spectroscopy and FT-IR spectroscopy. The intermolecular hydrogen-bonding interaction was evidenced by the fact that there were two characteristic bands at 2450 and 1920 cm^{-1} in the FT-IR spectra and the change in binding energy of N 1s by 0.72−0.88 eV relative to its reference compound *trans*-4-octyloxy-4′-stilbazole (**7**) were observed.

Introduction

Hydrogen-bonding interaction not only plays an important role in biological systems but also serves as a key driving force to assemble molecules to form liquid-crystalline materials. A large number of supramolecular liquid crystals have been built based on hydrogen-bonding interaction to date.[1−3] These supramolecular liquid crystals include a variety of families such as dimer, trimer, side-chain, etc.; however, main-chain linear hydrogen-bonded polymer is a class of important supramolecular liquid crystals. Before the pioneering work done by Fréchet[4,5] on hydrogen-bonded liquid crystals, there are only a few limited examples of the liquid crystals formed by identical molecules through *homo*-intermolecular hydrogen bond. For example, carboxylic acids including 4-alkoxybenzoic acids[6] and *trans*-*p*-methoxy- and ethoxycinnamic acids[7] dimerize through intermolecular hydrogen bonds and thus induce liquid crystallinity. Other examples on liquid crystals developed by identical amphiphilic species, such as carbohydrates,[8,9] polyols,[10,11] etc., were also reported. Kato and Fréchet[4] first exploited two different and independent components to generate liquid crystals through intermolecular *hetero*-hydrogen-bonding interaction, and this concept in turn resulted in numerous findings of such supramolecular liquid crystals.[12−18] On the basis of the above strategy, Griffin et al.[19−22] studied extensively main-chain linear hydrogen-bonded liquid crystals generated by bipyridyl derivatives and aromatic dicarboxylic acids. Moreover, the mesogenic phases of these complexes could be governed through specific structural modification such as substitution at the rigid moieties of the proton donor.[23] Recently, Lee et al. reported that polyoxyethylene-spacered bis(biphenyl) dicarboxylic acid and bipyridine formed hexagonal columnar and bicontinuous cubic liquid crystals.[24] Besides the liquid crystals formed by single hydrogen-bonding interaction, Lehn reported triple hydrogen-bonding complementary molecules which are capable of undergoing supramolecular polymerization via triple hydrogen-bonding interaction to induce main-chain thermotropic or lyotropic liquid crystals.[25] However, these reported main-chain supramolecular liquid crystals always consist of two complementary bifunctional monomers, a proton donor and a proton acceptor, which hold together through the intermolecular hydrogen bonds. To the best of our knowledge, no example was reported on main-chain liquid crystals generated by identical molecules through single *hetero*-intermolecular hydrogen-bonding interaction (Scheme 1).

Herein we wish to report the first main-chain liquid-crystalline polymers through the intermolecular hydrogen-bonding interaction among *single and identical* component bearing both donor and acceptor rigid groups instead of traditional entities consisting of two *different* and *independent* components. This type of molecular "complexes" exhibited mesogenic phases through the intermolecular hydrogen-bonding interaction. The mesogenic properties were characterized by differential scanning calorimetry (DSC) and polarized microscopy. Their hydrogen-bonding interaction was also studied by X-ray photoelectron spectroscopy (XPS) and FT-IR spectroscopy.

Experimental Section

General Data. All reactions were carried out under nitrogen. Commercially available reagents and solvents were used as received. ^{1}H NMR spectra were recorded on a Bruker DCR 400 spectrometer in $CDCl_3$ (unless otherwise stated) and tetramethylsilane (TMS) was used as a standard. EIMS and HRMS spectra were recorded on a Micromass 7034E mass

* To whom correspondence should be addressed. Tel: +65-6874-8145. Fax: +65-6872-7528. E-mail: cb-he@imre.a-star.edu.sg.
[†] Institute of Materials Research & Engineering.
[‡] Nanyang Technological University.

10.1021/ma047999l CCC: $30.25
Published on Web 01/27/2005

Scheme 1

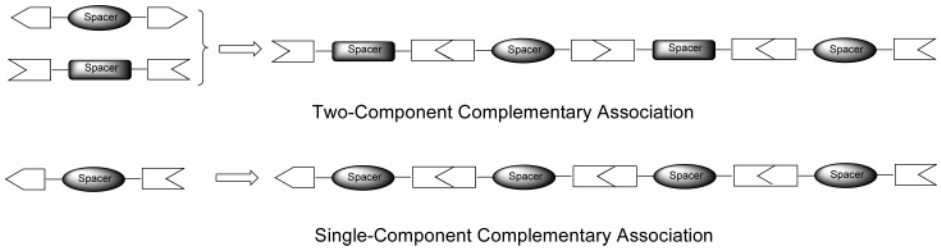

spectrometer. Elemental analysis was conducted on a Perkin-Elmer 240C elemental analyzer for C, H, and N determination. Infrared spectra (KBr, pellets) were measured on a Perkin-Elmer Fourier transform infrared (FT-IR) spectrophotometer 2000. X-ray photoelectron spectroscopy measurements were carried out on an ESCALAB 220i-XL spectrometer using a Mg Kα X-ray source (1253.6 eV). The X-ray source was run at 12 kV and 10 mA. All core-level spectra were referenced to the C 1s neutral carbon peak at a binding energy of 285.0 eV in order to compensate for surface charge effects. The pressure in the analysis chamber was maintained under ultrahigh vacuum at 10^{-9} mbar. Differential scanning calorimetry experiments were carried out on a TA Instrument DSC 2920 at a heating rate of 5 °C min^{-1} in nitrogen. Photomicrographs were taken on a Nikon OPTIPHOT2-POL polarizing optical microscope, equipped with a TMC-6RGB1/2″ color CCD camera and a temperature programmer TP-93. X-ray diffraction pattern was recorded on a Bruker GADDS X-ray diffractometer equipped with a hot stage using Cu Kα radiation wavelength (λ = 1.54 Å).

General Synthetic Procedure of 3a—d. A mixture of methyl *p*-hydroxybenzoate (3.0 mmol), alkyl dibromide (15.0 mmol), and NaOH (1.2 g, 3.0 mmol) in ethanol (250 mL) was heated at reflux for 8 h. After the reaction was complete, solvent was removed under reduced pressure. The oily liquid was dissolved in chloroform and then washed with water and dried with anhydrous $MgSO_4$. The drying agent was filtered off, and organic solvent was distilled off. The unreacted alkyl dibromide was removed under vacuum. The oily residue was chromatographed on silica gel using chloroform and methanol as eluent to afford compound **3**.

Methyl 4-(6-Bromohexyloxy)benzoate (3a). Yield: 55%. Mp: 42−44 °C. FT-IR (KBr): 3075, 3011, 2939, 2877, 2862, 1724, 1679, 1607, 1509, 1475, 1466, 1435, 1417, 1394, 1368, 1316, 1254, 1191, 1170, 1106, 1028, 1010, 997, 956, 848, 736, 726, 699, 645, 516 cm^{-1}. ^{1}H NMR: δ 7.97 (d, 2 H, J = 8.7 Hz), 6.90 (d, 2 H, J = 8.7 Hz), 4.00 (t, 2 H, J = 6.4 Hz), 3.88 (s, 3 H), 3.41 (t, 2 H, J = 6.7 Hz), 1.92−1.79 (m, 4 H), 1.51−1.49 (m, 4 H). MS (EI, *m/z*): 315 (M^+). Anal. Calcd for $C_{14}H_{19}BrO_3$: C, 53.35; H, 6.08; Found: C, 53.40; H, 5.94.

Methyl 4-(8-Bromooctyloxy)benzoate (3b). Yield: 53%. Mp: 48−50 °C. FT-IR (KBr): 3075, 3010, 2960, 2937, 2877, 2857, 1724, 1678, 1608, 1509, 1474, 1464, 1435, 1417, 1395, 1317, 1281, 1255, 1227, 1193, 1170, 1107, 1022, 956, 847, 767, 732, 722, 700, 650, 632, 517 cm^{-1}. ^{1}H NMR: δ 7.98 (d, 2 H, J = 9.0 Hz), 6.90 (d, 2 H, J = 9.0 Hz), 4.00 (t, 2 H, J = 6.4 Hz), 3.88 (s, 3 H), 3.41 (t, 2 H, J = 6.8 Hz), 1.90−1.76 (m, 4 H), 1.52−1.42 (m, 4 H), 1.42−1.30 (m, 4 H). MS (EI, *m/z*): 343 (M^+). Anal. Calcd for $C_{16}H_{23}BrO_3$: C, 55.98; H, 6.75; Found: C, 56.10; H, 7.01.

Methyl 4-(10-Bromodecyloxy)benzoate (3c). Yield: 60%. Mp: 61−62 °C. FT-IR (KBr): 3076, 3015, 2960, 2938, 2919, 2879, 2849, 1725, 1678, 1609, 1509, 1473, 1464, 1435, 1416, 1394, 1317, 1281, 1259, 1217, 1191, 1171, 1107, 1036, 1013, 957, 850, 767, 730, 720, 700, 646, 632, 517 cm^{-1}. ^{1}H NMR: δ ^{1}H NMR: δ 7.97 (d, 2 H, J = 8.8 Hz), 6.90 (d, 2 H, J = 8.8 Hz), 4.00 (t, 2 H, J = 6.5 Hz), 3.88 (s, 3 H), 3.41 (t, 2 H, J = 6.8 Hz), 1.89−1.76 (m, 4 H), 1.49−1.40 (m, 4 H), 1.40−1.280 (m, 8 H). MS (EI, *m/z*): 371 (M^+). Anal. Calcd for $C_{18}H_{27}BrO_3$: C, 58.22; H, 7.33; Found: C, 58.40; H, 7.50.

Methyl 4-(12-Bromododecyloxy)benzoate (3d). Yield: 56%. Mp: 68−70 °C. FT-IR (KBr): 3077, 3014, 2961, 2917, 2879, 2849, 1724, 1678, 1609, 1509, 1473, 1464, 1435, 1394, 1316, 1282, 1258, 1210, 1192, 1171, 1107, 1027, 1011, 958, 850, 834, 767, 729, 720, 701, 647, 632, 517 cm^{-1}. ^{1}H NMR: δ 7.97 (d, 2 H, J = 8.7 Hz), 6.90 (d, 2 H, J = 8.7 Hz), 4.00 (t, 2 H, J = 6.5 Hz), 3.88 (s, 3 H), 3.41 (t, 2 H, J = 7.0 Hz), 1.89−1.75 (m, 4 H), 1.50−1.39 (m, 4 H), 1.39−1.24 (m, 12 H). MS (EI, *m/z*): 399 (M^+). Anal. Calcd for $C_{20}H_{31}BrO_3$: C, 60.15; H, 7.82; Found: C, 60.07; H, 7.90.

General Synthetic Procedure for 5a—d. A mixture of compound **3** (0.50 mmol), *trans*-4-hydroxy-4′-stilbazole **4** (1.0 mmol), and anhydrous K_2CO_3 (1.38 g, 1.0 mmol) in dry DMF (50 mL) was heated at 65−70 °C for 6 h. The reaction mixture was cooled to room temperature and poured into ice−water with stirring. The suspension was filtered and the residue was washed with water. The semisolid was dissolved in chloroform. The organic phase was washed with water and brine and then dried over anhydrous sodium sulfate. The residue obtained after solvent removal was chromatographed on silica gel with chloroform/methanol (98:2) as eluent. The product was obtained as a pale yellow solid.

Methyl 4-{[6-(4-Stilbazoyl)]hexyloxy}benzoate (5a). Yield: 57%. Yield: Mp: 143−144 °C. FT-IR (KBr): 3052, 3022, 2941, 2913, 2866, 1725, 1607, 1590, 1551, 1509, 1475, 1435, 1416, 1397, 1316, 1281, 1252, 1191, 1171, 1108, 1020, 970, 958, 850, 834, 825, 767, 700, 552, 544 cm^{-1}. ^{1}H NMR: δ 8.55 (d, 2 H, J = 5.8 Hz), 7.98 (d, 2 H, J = 8.7 Hz), 7.47 (d, 2 H, J = 8.7 Hz), 7.33 (d, 2 H, J = 5.8 Hz), 7.25 (d, 1 H, J = 16.3 Hz), 6.90 (d, 4 H), 6.87 (d, 1 H, J = 16.3 Hz), 4.00 (q, 4 H), 3.88 (s, 3 H), 1.82 (br., 4 H), 1.55−1.50 (br. m, 4 H). MS (EI, *m/z*): 431 (M^+). Anal. Calcd for $C_{27}H_{29}NO_4$: C, 75.15; H, 6.77; N, 3.25; Found: C, 75.32; H, 6.99; N, 3.40.

Methyl 4-{[8-(4-Stilbazoyl)]octyloxy}benzoate (5b). Yield: 55%. Mp: 123−126 °C. FT-IR (KBr): 3052, 3021, 2937, 2922, 2876, 2858, 1726, 1607, 1590, 1551, 1509, 1475, 1435, 1415, 1397, 1315, 1280, 1256, 1171, 1108, 1032, 1011, 991, 970, 959, 849, 834, 825, 766, 700, 553, 545 cm^{-1}. ^{1}H NMR: δ 8.55 (dd, 2 H, J = 6.2 and 1.5 Hz), 7.98 (d, 2 H, J = 8.9 Hz), 9.47 (d, 2 H, J = 8.9 Hz), 7.33 (dd, 2 H, J = 6.2 and 1.5 Hz), 7.25 (d, 1 H, J = 16.2 Hz), 6.90 (d, 2 H, J = 8.9 Hz), 6.89 (d, 2 H, J = 8.9 Hz), 6.87 (d, 1 H, J = 16.2 Hz), 3.99 (q, 4 H), 3.88 (s, 3 H), 1.81 (m, 4 H), 1.55−1.44 (m, 4 H), 1.44−1.36 (m, 4 H). MS (EI, *m/z*): 459 (M^+). Anal. Calcd for $C_{29}H_{33}NO_4$: C, 75.79; H, 7.24; N, 3.05; Found: C, 75.89; H, 7.10; N, 2.98.

Methyl 4-{[10-(4-Stilbazoyl)]decyloxy}benzoate (5c). Yield: 58%. Mp: 136−138 °C. FT-IR (KBr): 3071, 3052, 3022, 2937, 2920, 2876, 2851, 1725, 1607, 1590, 1551, 1509, 1475, 1435, 1415, 1395, 1317, 1281, 1255, 1191, 1171, 1108, 1047, 1019, 969, 959, 849, 834, 824, 766, 700, 648, 553, 545 cm^{-1}. ^{1}H NMR: δ 8.54 (dd, 2 H, J = 6.2 and 1.6 Hz), 7.98 (d, 2 H, J = 8.9 Hz), 7.47 (d, 2 H, J = 8.7 Hz), 7.33 (dd, 2 H, J = 6.2 and 1.6 Hz), 7.25 (d, 1 H, J = 15.9 Hz), 6.91 (d, 2 H, J = 8.7 Hz), 6.90 (d, 2 H, J = 8.9 Hz), 6.87 (d, 1 H, J = 15.9 Hz), 3.99 (q, 4 H), 3.88 (s, 3 H), 1.80 (m, 4 H), 1.52−1.42 (m, 4 H), 1.42−1.29 (br. s, 8 H). MS (EI, *m/z*): 487 (M^+). Anal. Calcd for $C_{31}H_{37}NO_4$: C, 76.36; H, 7.65; N, 2.87; Found: C, 76.30; H, 7.80; N, 2.93.

Methyl 4-{[12-(4-Stilbazoyl)]dodecyloxy}benzoate (5d). Yield: 61%. Mp: 136−137 °C. FT-IR (KBr): 3052, 3022, 2937, 2919, 2876, 2849, 1725, 1608, 1590, 1551, 1510, 1474, 1464, 1435, 1414, 1395, 1317, 1280, 1257, 1191, 1171, 1108, 1030, 1011, 1003, 969, 959, 851, 834, 824, 766, 700, 648, 553, 544 cm^{-1}. ^{1}H NMR: δ 8.54 (dd, 2 H, J = 6.0 and 1.4 Hz), 7.97 (d, 2 H, J = 9.1 Hz), 9.47 (d, 2 H, J = 8.9 Hz), 7,33 (dd, 2 H, J = 6.0 and 1.4 Hz) 7.25 (1 H, J = 16.2 Hz), 6.91 (d, 2 H, J = 9.1 Hz), 6.90 (d, 2 H, J = 8.9 Hz), 6.87 (d, 1 H, J = 16.2 Hz), 3.99

(q, 4 H), 3.88 (s, 3 H), 1.79 (m, 4 H), 1.51−1.41 (m, 4 H), 1.41−1.25 (m, 12 H). MS (EI, *m/z*): 515 (M^+). Anal. Calcd for $C_{33}H_{41}NO_4$: C, 76.86; H, 8.01; N, 2.72; Found: C, 76.98; H, 8.25; N, 2.89.

General Synthetic Procedure for 6a—d. Compound **5** (0.15 g) was added to a solution of 15% KOH in ethanol and water (v:v = 1:3). The suspension was refluxed gently for 5 h and then was cooled to ambient temperature. The mixture was filtered, and the residue was washed with water, ethanol, and chloroform. The solid was neutralized with hydrochloric acid at 0 °C and then filtered. The solid was washed with water, ethanol and chloroform and collected as a white or pale-yellow solid.

4-{[6-(4-Stilbazoyl)]hexyloxy}benzoic Acid (6a). Yield: 40%. FT-IR (KBr): 3068, 3028, 2941, 2866, 2421, 1929, 1698, 1631, 1599, 1575, 1509, 1474, 1418, 1396, 1315, 1281, 1250, 1166, 1106, 1064, 1017, 968, 956, 853, 831, 775, 697, 642, 634, 559, 546 cm^{-1}. ^1H NMR (DMSO-d_6): δ 8.49 (dd, 2 H, J = 4.6 and 1.6 Hz), 7.86 (dd, 2 H, J = 6.8 and 2.1 Hz), 7.53 (dd, 2 H, J = 6.7 and 2.2 Hz), 7.46 (dd, J = 4.6 and 1.6 Hz), 7.38 (d, 2 H, J = 16.3 Hz), 6.99 (d, 2 H, J = 16.3 Hz), 6.90−6.97 (m, 4 H), 4.07 (t, 2 H, J = 6.5 Hz), 4.04 (t, 2 H, J = 6.4 Hz), 1.82−1.69 (m, 4 H), 1.55−1.45 (m, 4 H). MS (EI, *m/z*): 417.50 (M^+). M_r Calcd for $C_{26}H_{27}NO_4$: 417.1940. Found (HRMS): 417.1944.

4-{[8-(4-Stilbazoyl)]octyloxy}benzoic Acid (6b). Yield: 38%. FT-IR (KBr): 3069, 3028, 2937, 2924, 2859, 2435, 1929, 1698, 1633, 1600, 1576, 1509, 1474, 1465, 1418, 1394, 1367, 1315, 1281, 1254, 1177, 1168, 1064, 1030, 991, 969, 956, 852, 830, 775, 698, 561, 546 cm^{-1}. ^1H NMR (DMSO-d_6): δ 8.47 (dd, 2 H, J = 4.5 and 1.4 Hz), 7.78 (dd, 2 H, J = 6.7 and 1.9 Hz), 7.52 (dd, 2 H, J = 6.7 and 1.9 Hz), 7.42 (dd, 2 H, J = 4.5 and 1.4 Hz), 7.35 (d, 2 H, J = 16.5 Hz), 6.98 (d, 2 H, J = 16.5 Hz), 6.93 (dd, 2 H, J = 6.7 and 1.9 Hz), 6.76 (d, 2 H, J = 6.7 and 1.9 Hz), 4.02 (t, 2 H, J = 6.4 Hz), 3.98 (t, 2 H, J = 6.4 Hz), 1.76−1.67 (m, 4 H), 1.50−1.40 (m, 4 H), 1.40−1.29 (m, 4 H). MS (EI, *m/z*): 445.55 (M^+). M_r Calcd for $C_{28}H_{31}NO_4$: 445.2253. Found (HRMS): 445.2257.

4-{[10-(4-Stilbazoyl)]decyloxy}benzoic Acid (6c). Yield: 42%. FT-IR (KBr): 3070, 3027, 2937, 2921, 2852, 2473, 1927, 1698, 1633, 1599,1576, 1509, 1474, 1418, 1394, 1315, 1281, 1251, 1166, 1106, 1065, 1045, 1016, 969, 956, 852, 831, 775, 697, 640, 633, 560, 546 cm^{-1}. ^1H NMR (DMSO-d_6): δ 8.48 (dd, 2 H, J = 4.6 and 1.5 Hz), 7.85 (dd, 2 H, J = 6.5 and 1.8 Hz), 7.51 (dd, 2 H, J = 6.6 and 1.6 Hz), 7.43 (dd, 2 H, J = 4.6 and 1.5 Hz), 7.35 (d, 2 H, J = 16.2 Hz), 6.97 (d, 2 H, J = 16.2 Hz), 6.93−6.96 (m, 4 H), 4.05 (t, 2 H, J = 6.4 Hz), 4.01 (t, 2 H, J = 6.4 Hz), 1.75−1.64 (m, 4 H), 1.48−1.38 (m, 4 H), 1.38−1.24 (m, 8 H). MS (EI, *m/z*): 473.30 (M^+). *Mr* Calcd for $C_{30}H_{35}NO_4$: 473.2566. Found (HRMS): 473.2568.

4-{[12-(4-Stilbazoyl)]dodecyloxy}benzoic Acid (6d). Yield: 44%. FT-IR (KBr): 3070, 3027, 2936, 2920, 2851, 2476, 1927, 1698, 1633, 1599, 1576, 1510, 1474, 1474, 1418, 1394, 1315, 1280, 1255, 1166, 1106, 1065, 1029, 1011, 1003, 970, 956, 854, 831, 775, 698, 641, 634, 560, 546 cm^{-1}. ^1H NMR (DMSO-d_6): δ 8.47 (dd, 2 H, J = 4.5 and 1.6 Hz), 7.85 (dd, 2 H, J = 6.8 and 2.1 Hz), 7.52 (dd, 2 H, J = 6.8 and 2.0 Hz), 7.42 (dd, 2 H, J = 4.5 and 1.6 Hz), 7.35 (d, 2 H, J = 16.5 Hz), 6.98 (d, 2 H, J = 16.5 Hz), 6.91−6.95 (m, 4 H), 4.04 (t, 2 H, J = 6.4 Hz), 4.01 (t, 2 H, J = 6.4 Hz), 1.77−1.62 (m, 4 H), 1.47−1.37 (m, 4 H), 1.37−1.20 (m, 16 H). MS (EI, *m/z*): 501.2 (M^+). M_r Calcd for $C_{32}H_{39}NO_4$: 501.2879. Found (HRMS): 501.2883.

Results and Discussion

Synthesis of Monomers. The synthetic route leading to donor−spacer−acceptor molecules is outlined in Scheme 2. Methyl *p*-hydroxybenzoate reacted with excess corresponding alkyl dibromide **2a**−**d** to afford monosubstitued **3a**−**d** as major products in 53−60 % after column chromatography. Compounds **6a**−**d** were obtained by reaction **3a**−**d** with *trans*-4-hydroxy-4′-stilbazole (**4**) in dimethylacetamide (DMF) in the presence of anhydrous potassium carbonate, followed by hydrolysis in aqueous NaOH/ethanol and subsequent

Scheme 2. Synthesis of Donor−Spacer−Acceptor Molecules[a]

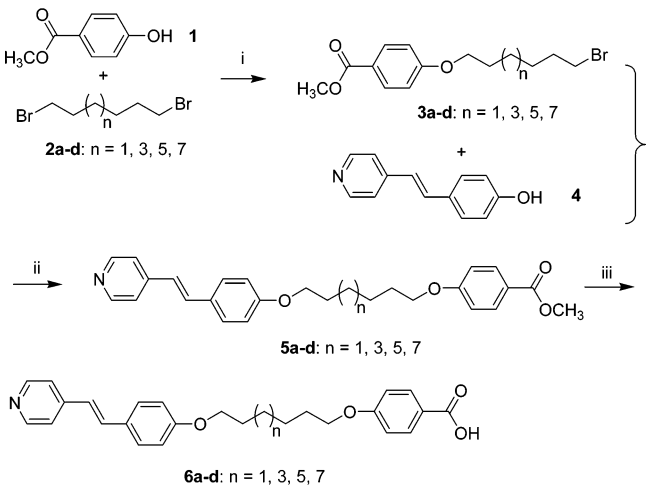

[a] Reagents and conditions: (i) NaOH, ethanol, reflux; (ii) K_2CO_3, DMF, 65-70 °C; (iii) NaOH, ethanol/H_2O, reflux, and then HCl.

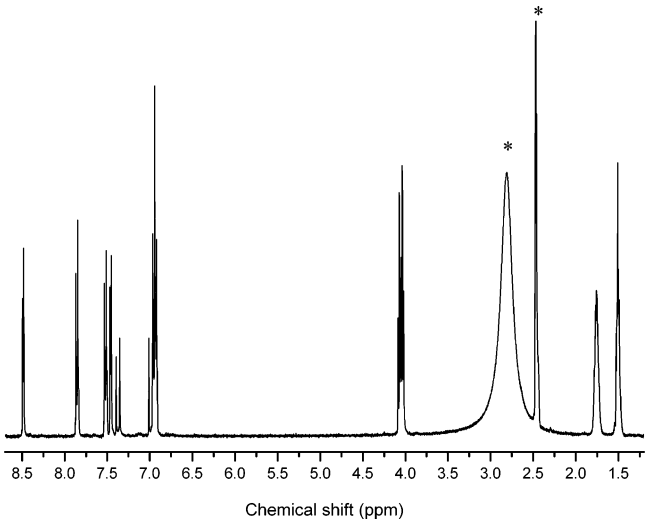

Figure 1. ^1H NMR spectrum of **6a** in $(CD_3)_2SO$ at 125 °C. (∗) residual water and undeuterated DMSO.

acidification with hydrochloric acid. The structures of all intermediates and final products **6a**−**d** were characterized unambiguously by ^1H NMR, FT-IR, mass spectra and elemental analyses. Because of the extremely low solubility of **6a**−**d** in common organic solvents at ambient temperature, their ^1H NMR spectra were therefore measured in deuterated dimethyl sulfoxide (DMSO-d_6) at 125 °C. The ^1H NMR spectrum of **6a**, as an example, is shown in Figure 1.

Liquid Crystallinity. Stilbazole-containing derivatives are frequently employed as a mesogenic core to construct the hydrogen-bonded supramolecular liquid crystals,[4,5,26,27] but these liquid crystals are always built by two or more independent and different complementary components through the intermolecular hydrogen-bonding interaction. For example, the complexes of benzocrown-containing stilbazole[28] or alkoxy-substituted stilbazole[4,29] with mono- or dicarboxylic acids formed mesogenic phases. Polyoxyethylene-spacered bis(stilbazole) derivatives could also produce a liquid-crystalline network with appropriate proton donors.[30] In our cases, however, being essentially different from the reported binary or tertiary complexes systems, **6a**−**d** are ex-

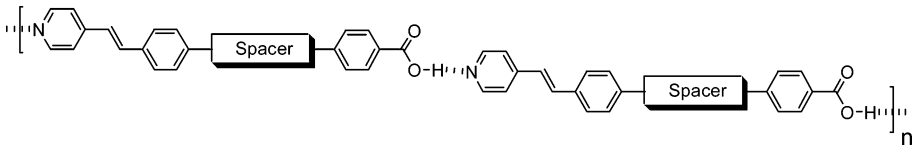

Figure 2. Supramolecular polymer built through the intermolecular hydrogen-bonding interaction among identical molecules **6a**−**d**.

Table 1. Thermal Behaviors of "Complexes" Formed by 6a−d[a]

	phase transition behavior									
complexes	heating			cooling						
6a	K	292/287	I	I	278/272(84.0)	S_B	194/192(22.5)	K		
6b	K	271/268	I	I	262/261(74.1)	S_B	203/202(8.5)	K_1	133/132(18.1)	K_2
6c	K	250/249	I	I	242/241(77.4)	S_B	229/229(9.8)	S_X[b]	175/175(43.6)	K
6d	K	239/238	I	I	232/232 (110.3)	S_B	183/182(34.1)	K		

[a] Transition temperatures (°C) are taken from the first and second run. Enthalpies of transition (J/g, in parentheses); K, crystalline; S, smectic, and I, isotropic. [b] S_X is an unidentified higher order smectic phase.

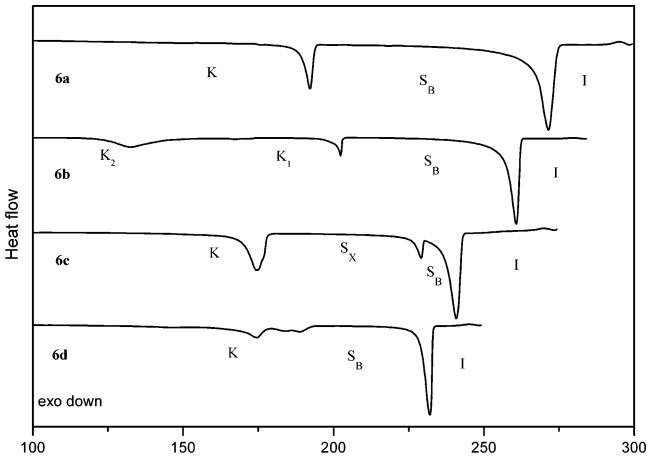

Figure 3. DSC thermograms of compounds **6a**−**d** on the second cooling.

pected to directly form hydrogen-bonded polymers alone without the aid of the second complementary component as shown in Figure 2. This is because the molecules **6a**−**d** consist of two rigid moieties that act as a proton donor (benzoic acid) and a proton acceptor (stilbazoyl moiety). The molecules will link the two rigid heads together via the intermolecular hydrogen-bonding interaction. Thus, differential scanning calorimetry (DSC) was performed to examine whether these "complexes" formed by an identical single-component generate a thermotropic liquid crystal similar to traditional two-component complexes. The DSC curves of the second cooling are shown in Figure 3, and their phase transition temperatures are summarized in Table 1.

From the DSC graphs of **6a**−**d**, we observed two or three main exothermic peaks on the second cooling, indicating the presence of phase-transition. The phase-transition was also studied using polarizing optical microscopy. The mosaic textures were observed for all compounds **6a**−**d** on cooling. As examples, polarizing photomicrographs of compounds **6c** and **6d** on cooling are given in Figure 4. A mosaic texture of a smectic B (S_B) phase was observed for compound **6d** at 232 °C on cooling. Similarly, compound **6c** displayed a mosaic texture of S_B at 235 °C on cooling. The relatively lower crystallization enthalpy change compared to that for isotropic to mesophase is indicative of a higher order smectic phase. In addition, the mosaic texture is a very common characteristic appearance of the S_B phase, particularly for materials with a direct S_B transition

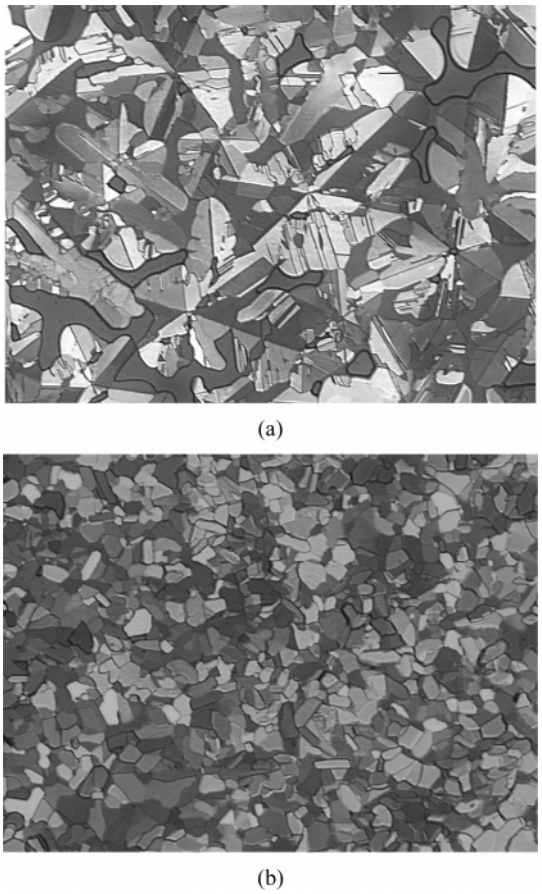

Figure 4. Optical texture of (a) smectic B phase of **6c** on cooling at 235 °C and (b) smectic B phase of **6d** on cooling at 232 °C.

from the isotropic melt.[31] Thus, we examined the X-ray diffraction of compounds **6a**−**d** at elevated temperatures to identify the exact liquid phase using **6d** as an example. Figure 5 shows the variable-temperature wide-angle X-ray scattering (WAXS) of compound **6d** when it was slowly cooled from its isotropic state. The scattering at 5.95° (2θ) is due to the scattering from the sample holder (glass tube). A strong sharp scattering at 4.85° (2θ) accompanying with a strong diffraction at $2\theta = 20.0°$ at 210 °C was observed. The strong scattering of 4.85° corresponds to the d spacing of 18.4 Å, being a second-order diffraction peak. The higher order smectic phases include S_B, S_E, S_F, S_G, S_H, S_I, etc. As reported,[32] a high order smectic phase would show a strong inner

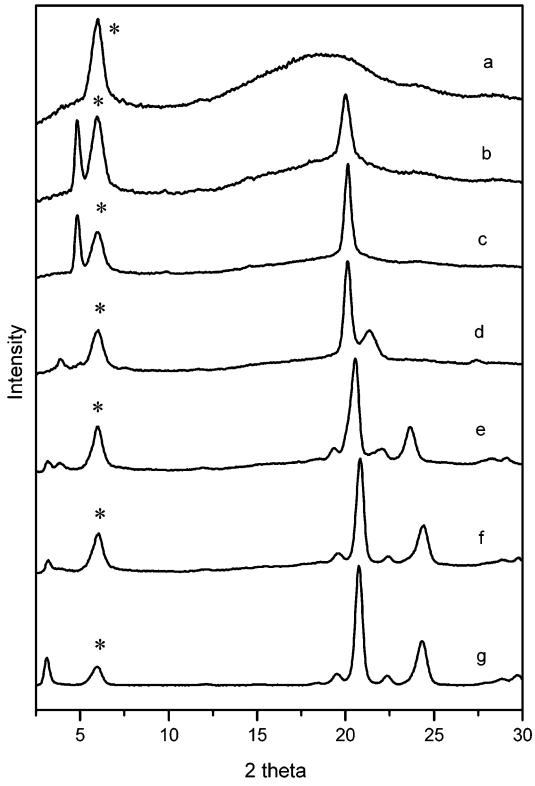

Figure 5. X-ray diffraction pattern of compound **6d** at (a) 240, (b) 210, (c) 190, (d) 180, (e) 160, and (f) 25 °C, on cooling, and (g) 25 °C before heating. (∗) The diffraction peak at $2\theta = 5.95°$ is from the glass sample holder. The intensity is offset for clarity.

diffraction and one or several strong outer diffraction peaks. The number of outer diffraction peaks in particular depends on the type of the smectic phase. In our case, the presence of a single strong sharp outer diffraction (20°) indicates that a S_B phase is present[32b−c] because S_E, S_G, S_H, and S_I show several sharp outer diffraction peaks, and S_F only shows a diffuse outer ring besides having a strong inner diffraction.[32d,33] When the temperature cooled to 180 °C, **6d** started to crystallize as observed that one diffraction peak at $2\theta = 21.4°$ emerged and the diffraction peak $2\theta = 4.85°$ became very weak and finally disappeared at 160 °C. In fact, the crystallization process of **6d** at this temperature range could be also observed clearly by using polarizing optical microscopy. The whole profiles of WAXS pattern of **6d** at room temperature before and after heating (curves g an f in Figure 5, respectively) was very similar, suggesting that "complex" **6d** is stable in the range of the experimental temperature limits.

To compare the relative thermal stability and reversibility of "complexes" **6a**−**d** with traditional two-component complexes, multiple cycles of **6a**−**d** from room temperature to isotropic phase were conducted by DSC. Similar to two or three-component complexes,[34] the phase transition temperatures of **6a**−**c**, on the first cooling correspond well to those on the second cooling, indicating the liquid crystals are quite stable and reproducible. However, the slight drop of transition temperature for **6a** is possibly due to the high melting point, thus leading to probable decomposition. The length of the flexible alkyloxy chain spacer between the donor and the acceptor in **6a**−**d** has an impact on the melting and mesophase transition temperature (Figure 6). For example, it was observed that the melting

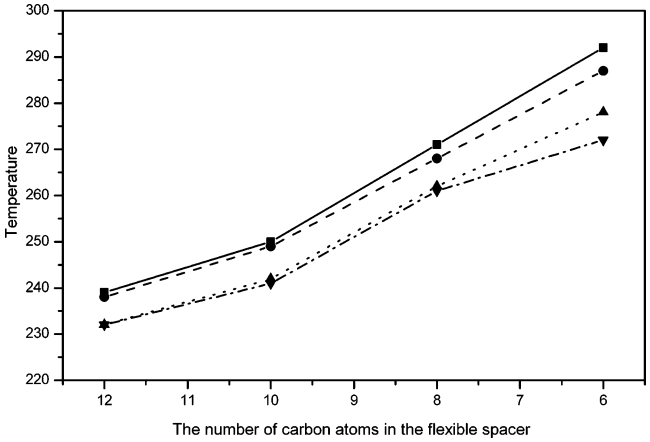

Figure 6. Relationship of length of the flexible spacer and the phase-transition temperatures: solid line, first heating; dashed line, second heating; dotted line, first cooling; dot-dash line: second cooling.

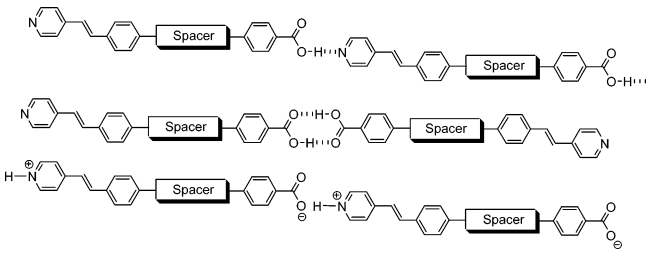

Figure 7. Possible entities present in **6a**−**d**.

temperatures of **6a**−**d** decreased gradually with the increase in length of the flexible spacer both in the first heating and in the second heating; likewise, the mesophase transition temperatures of **6a**−**d** were decreased steadily with the increase in length of the flexible spacer both in the first cooling and in the second cooling. These facts suggest that the phase-transition temperature could be controlled through adjusting the length of the spacer between donor and acceptor moieties.

XPS and FT-IR Spectroscopic Studies: Due to the presence of complementary functional groups (acidic −COOH group and basic pyridine group) in the same molecule, **6a**−**d** are likely to exist as three entities including a carboxylic acid dimer, a hydrogen-bonded molecular complex, and probably, a zwitterionic structure. Similar to amino acids, the coexistence of two functional groups in the same molecule would lead to the formation of zwitterionic structure (Figure 7). Thus, we examined the binding energy of N 1s using X-ray photoelectron spectroscopy as the binding energy of N 1s is very sensitive to environmental pertubration.[35] For example, free, hydrogen-bonded or protonated nitrogen would result in different binding energies. The XPS spectra are given in Figure 8 and the binding energies of N 1s of **6a**−**d** as well as their differences with a reference compound *trans*-4-octyloxy-4′-stilbazole (**7**) are summarized in Table 2. The binding energies of **6a**−**d** ranged from 399.24 to 399.40 eV, being larger by 0.72−0.88 eV than that of the "neutral" reference **7** in which neither intramolecular nor intermolecular hydrogen bond exists. In principle, the formation of hydrogen bond or protonated nitrogen leads to an upshift of the binding energy of N 1s due to the decrease in electron density in nitrogen atom. Since nitrogen atom could be involved in hydrogen-bonding or ionic bonding interaction (zwitterionic structure), the magnitude of change in the

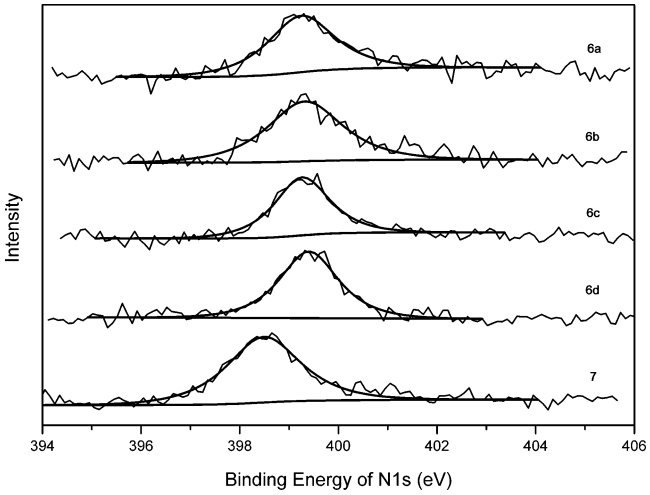

Figure 8. XPS graph of N 1s of compounds **6a**−**d** and **7**.

Table 2. Binding Energy of N 1s of 6a−d and the Difference in Binding Energy of N 1s with That of Ref 7[a]

	N 1s (eV)	ΔN 1s (eV)
6a	399.40	0.88
6b	399.26	0.74
6c	399.32	0.80
6d	399.24	0.72
7	398.52	

[a] $\Delta N\ 1s = N\ 1s_{complex} - N\ 1s_7$.

binding energy of N 1s correlates to the nature of the interaction. For the hydrogen-bonded nitrogen, the change in the binding energy of N 1s relative to its free state is usually less than 1.0 eV.[36−40] In contrast, for protonated nitrogen, its binding energy change with respect to its free state is more than 2.0 eV.[38,40] Subsequently, the change ranging from 0.72 to 0.88 eV in binding energy suggests that the supramolecular assembly synthon of **6a**−**d** is a hydrogen-bonded entity rather than a zwitterionic entity in nature.

The FT-IR spectra of **6a**−**d** together with two reference compounds **7** and 4-hexyloxybenzoic acid (**8**) are shown in Figure 9, parts a and b. For the reference compound **8**, it prefers to form a hydrogen-bonded dimer, and three broad stretching bands of hydroxyl group are therefore observed at around 3000, 2670, and 2560 cm^{-1} in its FT-IR spectrum. As can be seen clearly from Figure 9, parts a and b, **6a**−**d** showed a similar IR spectral profile, but in comparison with **8**, the stretching bands of hydroxyl group shifted to the lower wavenumber at ca. 2450 and 1920 cm^{-1} (Figure 9a) which are assigned to be the characteristic bands of the hydrogen-bonding interaction (O═C−O−H···N).[41] Moreover, no specific band from dimerized carboxylic acid was observed, deducing that the carboxylic dimer was absent or negligible. This is indeed consistent with the above argument derived from XPS that **6a**−**d** is comprised of hydrogen-bonded entities. In addition, for the carbonyl stretching absorption (1698 cm^{-1}), **6a**−**d** displayed a higher wavenumber by 16 cm^{-1} compared to **8** (1682 cm^{-1}). The carbonyl oxygen was not involved in the formation of the hydrogen bonds (O═C−O−H···N) in **6a**−**d**, as a result, leading to an increase of electron density in oxygen and subsequently a higher wavenumber shift in their FT-IR spectra. The protonated pyridine absorption usually resulted in a higher wavenumber shift relative to its free state.[38] For example, protonated poly(4-vinylpyridine) has a higher wavenumber by 30

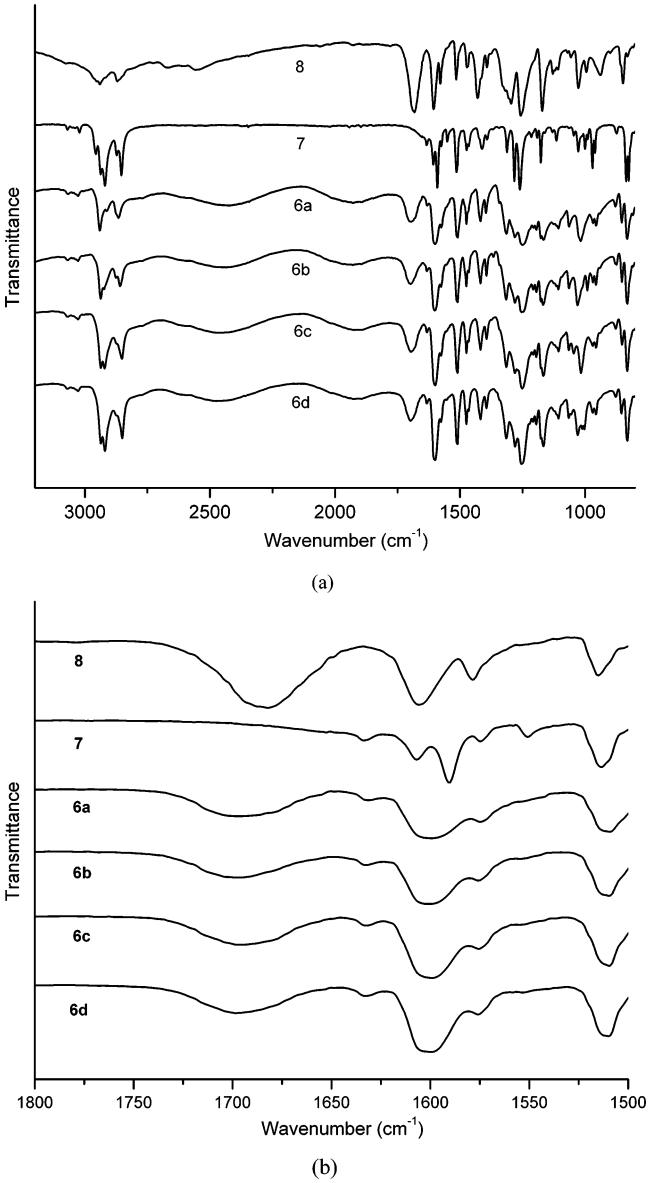

Figure 9. FT-IR spectra of compounds **6a**−**d**, **7**, and **8**: (a) 3200−800 cm^{-1} and (b) 1800−1500 cm^{-1}.

cm^{-1} more than its free state.[38] In our case, the pyridine absorption of **6a**−**d** at 1590 cm^{-1} moved to the band centered at 1599 cm^{-1}, and overlapped with a peak at 1607 cm^{-1} (Figure 9b). No appearance of a new relatively strong band at around 1620 cm^{-1} (The weak peak at 1633 cm^{-1} was attributed to the stretching absorption of CH═CH in stibazole), corresponding to a characteristic band of protonated pyridine, was observed, suggesting that the "complex" is formed through hydrogen-bonding interaction rather than through ionic interaction. Therefore, we can conclude that the upshift (less 1 eV) of the binding energy of N 1s in XPS spectra when compared to that of the "neutral" reference **7** and the characteristic bands as observed at 2450 and 1920 cm^{-1} in their FT-IR spectra collectively confirm the existence of the intermolecular hydrogen-bonding interaction in **6a**−**d**.

Conclusions

We have demonstrated in this paper that the synthesis of a series of donor−spacer−acceptor molecules could be readily achieved. These molecules self-assembled

through the intermolecular hydrogen-bonding interaction to give rise to molecular "complexes" and exhibited thermotropic liquid crystallinity. The alkyloxy-chain flexible spacers in **6a**−**d** correlated to their thermal behaviors, especially for the mesophase transition and melting temperatures. The phase transition temperatures decreased steadily with the increase in the spacer length. The XPS and FT-IR investigations confirmed that the interaction among the molecules of **6a**−**d** belonged to the hydrogen-bonding interaction. There have been reported a number of main-chain supramolecular liquid crystalline polymers which derived from self-assembly of two different bifunctional molecules either via single hydrogen-bonding interaction[19−23] or via multiple hydrogen-bonding interaction,[25] while in this paper we demonstrated a method to build main-chain liquid-crystalline polymers by self-assembling identical molecules bearing both a donor and an acceptor groups through a single hydrogen-bonding, it allows us to develop more interesting hydrogen-bonded liquid-crystalline polymers beyond those reported in this paper, for example, liquid-crystalline networks.

Acknowledgment. Financial support for the work was provided by Institute of Materials Research and Engineering (IMRE). We thank Mr Cai Jianwei in the Characterization and Material Science Cluster in IMRE, for his technical assistance in XPS.

References and Notes

(1) Paleos, C. M.; Tsiourvas, D. *Liq. Cryst.* **2001**, *28*, 1127 and references therein.
(2) Paleos, C. M.; Tsiourvas, D. *Angew. Chem., Int. Ed. Engl.* **1995**, *34*, 1696.
(3) (a) Kato, T. In *Handbook of Liquid Crystals*; Demus, D., Goodby, J., Gray, G. W., Spiess, H. W., Vill, V., Eds.; Wiley-VCH: Weinheim, Germany, 1998; pp 969−979. (b) Blunk, D.; Praefcke, K.; Vill, V. In *Handbook of Liquid Crystals*; Demus, D., Goodby, J., Gray, G. W., Spiess, H. W., Vill, V., Eds.; Wiley-VCH: Weinheim, Germany, 1998; pp 305−340. (c) Lu, X.; He, C.; Griffin, A. C. *Macromolecules* **2003**, *36*, 5195. (d) Lu, X.; He, C.; Terrell, C. D.; Griffin, A. C. *Macromol. Chem. Phys.* **2002**, *203*, 85. (e) Kato, T.; Matsuoka, T.; Nishii, M.; Kamikawa, Y.; Kanie, K.; Nishimura, T.; Yashima, E.; Ujiie, S. *Angew. Chem., Int. Ed.* **2004**, *43*, 1969. (f) Sautter, A.; Thalacker, C.; Würthner, F. *Angew. Chem., Int. Ed.* **2001**, *40*, 4425. (g) Lee, M.; Cho, B.-K.; Kim, H.; Zin, W.-C. *Angew. Chem., Int. Ed. Engl.* **1998**, *37*, 638. (h) Lehn, J.-M. *Poly Int.* **2002**, *51*, 825.
(4) Kato, T.; Fréchet, J. M. J. *J. Am. Chem. Soc.* **1989**, *111*, 8533.
(5) Kato, T.; Fréchet, J. M. J. *Macromolecules* **1989**, *22*, 3818.
(6) Gray, G. W. Jones, B. *J. Chem. Soc.* **1953**, 4179.
(7) Gray, G. W.; Jones, B. *Molecular Structure and Liquid Crystals*; Academic Press: London, 1967; p 61 and references therein.
(8) Jeffrey, G. A. *Acc. Chem. Res.* **1986**, *19*, 168.
(9) Jeffrey, G. A.; Wingert, L. M. *Liq. Cryst.* **1992**, *12*, 179.
(10) Praefcke, K.; Kohne, B.; Diele, S.; Pelzl, D.; Kjaer, A. *Liq. Cryst.* **1992**, *11*, 1.
(11) Frank, H.; Carsten, T.; Horst, Z. *Angew. Chem., Int. Ed. Engl.* **1991**, *30*, 440.
(12) Kato, T.; Fréchet, J. M. J. Wilson, P. G.; Saito, T.; Uryu, T. Fujishima, A.; Jin, C.; Kaneuchi, F. *Chem. Mater.* **1993**, *5*, 1094.
(13) Willis, K.; Price, D. J.; Adams, H.; Ungar, G.; Bruce, D. W. *J. Mater. Chem.* **1995**, *5*, 2195.
(14) Price, D. J.; Willis, K.; Richardson, T.; Adams, H.; Ungar, G.; Bruce, D. W. *J. Mater Chem.* **1997**, *7*, 883.
(15) Willis, K.; Luckhurst, J. E.; Price, D. J.; Fréchet, J. M. J.; Kihara, H.; Kato, T.; Ungar, G.; Bruce, D. W. *Liq. Cryst.* **1996**, *21*, 585.
(16) Yu, L. J.; Wu, J. M.; Wu, S. L. *Mol. Cryst. Liq. Cryst.* **1991**, *198*, 407.
(17) Yu, L. J.; Pan, J. S. *Liq. Cryst.* **1993**, *14*, 829.
(18) Kato, T.; Wilson, P. G.; Fujishima, A.; Fréchet, J. M. J. *Chem. Lett.* **1990**, 2003.
(19) Pourcain, C. B. S.; Griffin, A. C. *Macromolecules* **1995**, *28*, 4116.
(20) Bladon, P.; Griffin, A. C. *Macromolecules* **1993**, *26*, 6604.
(21) He, C. B.; Donald, A. M.; Griffin, A. C.; Waigh, T.; Windle, A. H. *J. Polym. Sci., Polym. Phys. Ed.* **1998**, *36*, 1617.
(22) Lee, C.-M.; Jariwala, C. P.; Griffin, A. C. *Polymer* **1994**, *35*, 4550.
(23) Lee, C.-M.; Griffin, A. C. *Macromol. Symp.* **1997**, *117*, 281.
(24) Lee, M.; Cho, B. K.; Kang, Y. S.; Zin, W. C. *Macromolecules* **1999**, *32*, 8531.
(25) (a) Lehn, J.-M. *Adv. Mater.* **1990**, *2*, 254. (b) Lehn, J.-M. *Chem. Commun.* **1994**, 197.
(26) Kato, T.; Fujishima, A.; Fréchet, J. M. J. *Chem. Lett.* **1990**, 919.
(27) Yu, L. J. *Liq. Cryst.* **1993**, *14*, 1303.
(28) Gündogan, B.; Ninnemans, K. *Liq. Cryst.* **2000**, *27*, 851.
(29) Kato, T.; Adachi, H.; Fujishima, A.; Fréchet, J. M. J. *Chem. Lett.* **1992**, 265.
(30) Kihara, H.; Kato, T.; Uryu, T.; Fréchet, J. M. J. *Chem. Mater.* **1996**, *8*, 961.
(31) Dierking, I. *Textures of Liquid Crystals*; Wiley-VCH: Weinheim, Germnay, 2003; pp 135−139 and references therein.
(32) (a) de Vries, A. *Mol. Cryst. Liq. Cryst.* **1973**, *24*, 337. (b) de Vries, A. *Chem. Phys. Lett.* **1974**, *28*, 252. (c) Hsu, C.-S.; Lin, J.-H.; Chou, L.-R.; Hsiue, G.-H. *Macromolecules*, **1992**, *25*, 7126. (d) Kelker, H.; Hatz, R. *Handbook of Liquid Crystals*; Verlag Chemie GmbH: Weinheim, Germany, 1980; pp 231−242.
(33) Krigbaum, W. R.; J. Watanabe, J.; Ishikawa, T. *Macromolecules* **1983**, *16*, 1271.
(34) Xu, J.; He, C.; Toh, K. C.; Lu, X. *Macromolecules* **2002**, *35*, 8846.
(35) Li, X.; Goh, S. H.; Lai, Y. H.; Wee, A. T. S. *Polymer* **2001**, *42*, 5463.
(36) Luo, X. F.; Goh, S. H.; Lee, S. Y.; Huan, Cha. *Macromol. Chem. Phys.* **1999**, *200*, 874.
(37) Goh, S. H.; Lee, S. Y.; Dai, J.; Tan, K. L. *Polymer* **1996**, *37*, 5305.
(38) Zhou, X.; Goh, S. H.; Lee, S. Y.; Tan, K. L. *Appl. Surf. Sci.* **1998**, *126*, 141.
(39) Zhou, X.; Goh, S. H.; Lee, S. Y.; Tan, K. L. *Polymer* **1998**, *39*, 3631.
(40) Luo, X. F.; Goh, S. H.; Lee, S. Y.; Tan, K. L. *Macromolecules* **1998**, *31*, 3251.
(41) Kumar, U.; Kato, T.; Uryu, T.; Fréchet, J. M. J. *J. Am. Chem. Soc.* **1992**, *114*, 6630.

MA047999L